Nanomaterials

DOI: 10.1002/anie.201209099

Graphene: Safe or Toxic? The Two Faces of the Medal

*Alberto Bianco**

carbon materials · graphene · materials science · nanotoxicity

Dedicated to Prof. Maurizio Prato on the occasion of his 60th birthday

Graphene is considered the future revolutionary material. For its development, it is of fundamental importance to evaluate the safety profile and the impact on health. Graphene is part of a bigger family which has been identified as the graphene family nanomaterials (GFNs). Clarifying the existence of multiple graphene forms allows better understanding the differences between the components and eventually correlating their biological effects to the physicochemical characteristics of each structure. Some in vitro and in vivo studies clearly showed no particular risks, while others have indicated that GFNs might become health hazards. This Minireview critically discusses the recent studies on the toxicity of GFNs to provide some perspective on the possible risks to their future development in materials and biomedical sciences.

1. Introduction

Graphene, the new allotrope of carbon, is defined as a single layer of monocrystalline graphite with sp^2-hybridized carbon atoms. Since the pioneering work by Novoselov and Geim,[1] graphene has emerged as a new carbon nanoform with great potential in many applications in materials science.[2] It is also gaining a lot of interest in the biomedical field as a new component for biosensors, tissue engineering, and drug delivery.[3–6] Very recently a road map for graphene has been proposed with the aiming of providing future directions for its development in the fields of electronics, photonics, composite materials, energy generation and storage, sensors and metrology, and biomedicine.[7]

One key paradigm is that nanosafety research must be part of the development of new nanotechnologies. As for all new types of nanomaterials, graphene is not devoid of possible risks to human health or the environment. Indeed, graphene cannot be excluded from this type of investigation when considering responsible use of this emerging nanomaterial, which is beginning to be produced in substantial amounts. However, before speaking of the "devil" it is of fundamental importance to explore the level of toxicity of graphene and to what degree it is safe. Resolving the safety and toxicity issues associated with this new nanomaterial will be not only beneficial to its integration into new composites, nanoelectronics, etc. but also in the case of possible biomedical applications, which are currently being explored. Recent reviews have already covered the biomedical potential of graphene and other grapheme-derived materials.[8,9] However, a limited amount of data exists in the literature on the impact of graphene on health and the environment.[10–14]

This review is summarizes the current state-of-the art on the toxicity studies of graphene and its related congeners, including graphene oxide (GO), reduced graphene oxide (rGO), few-layer graphene, graphene nanosheets and flakes, graphene ribbons and dots, all of which are part of the graphene family nanomaterials (GFNs). As the graphene family comprises these different members endowed with different chemicophysical characteristics, their toxicological profile is little understood and more thorough studies are required. What is emerging from the available results is a variety of effects which are strictly related to the nature of the graphene used. We will try to correlate these effects to the features of the different graphenes tested, with the goal of explaining the available data and providing an outlook on the potential future applications, particularly in the biomedical domain. It is evident that chemical modifications of graphene modulate the toxicity impact (see the following sections) as it has been also demonstrated for carbon nanotubes.[8,9,15] This is certainly a favorable point in the development of such types of nanomaterials in biomedicine. The recent findings on the possible biodegradability of GO is another positive factor which needs further exploration to assess the safe use of the graphene family members.[16] With the development of mass-scale production of graphene, the multiplication of their uses, and arrival in the marketplace, it is also essential to assess exposure under real conditions and fully understand the life cycle of this material.

[*] Prof. A. Bianco
CNRS, Institut de Biologie Moléculaire et Cellulaire
Laboratoire d'Immunopathologie et Chimie Thérapeutique
15 Rue René Descartes, 67084 Strasbourg (France)
E-mail: a.bianco@ibmc-cnrs.unistra.fr

2. Graphene Family Nanomaterials

Graphene is part of a bigger family that has been identified as GFNs. Identifying the existence of multiple graphene forms allows better recognition of the differences between the components of the family and eventually associating the toxic effects with the physicochemical characteristics of each family member. GFNs comprise single-layer graphene, few-layer graphene (2–10 graphene layers), GO (normally a single layer), rGO (normally a single layer), graphene nanosheets, ultrafine graphite (more than 10 sheets but below 100 nm in thickness), graphene ribbons, and graphene dots. Figure 1 shows the chemical structure of some GFNs.

Within each of these forms a variety of structures is possible. For example for GO, it is extremely difficult to describe at the molecular level the type, the degree, and the position of the oxygenated groups introduced during the process of graphite exfoliation.[17] Even more complicated is understanding what happens when GO is transformed under reductive conditions.[18,19] Are we able to reconstitute the intact graphitic plane? Are just the oxygen-containing groups simply eliminated? Are these functions replaced by the reducing reagents? All these issues are currently under investigation. Indeed, a thorough description of the different graphene forms is mandatory to elucidate their biological effects and to correlate them to the structure of the material.

In addition, a single graphene layer might have different dimensions in terms of surface area, thus allowing definition of small graphene flakes and large graphene sheets which might reach ten to a hundred square microns (Figure 2). The analysis of this parameter is also extremely important for the evaluation of the toxicity risks of GFNs.

A certain number of studies have been devoted to assess the in vitro and in vivo toxic effects of GFNs. Some of the studies clearly showed no particular risks while others have indicated that GFNs might become health hazards. Inhalation, for example, is one of the key routes of human exposure. Some GFNs have an aerodynamic size which can lead to inhalation and deposition within the respiratory tract with possible implications on the formation of granulomas and lung fibrosis.[20] However, the biological responses certainly vary depending on the number of layers, lateral size, stiffness, hydrophobicity, surface functionalization, dose administered, and purity of the material.[11–14] Not much is known about the possible differences in the biological behavior between large and small sheets of graphene, or even few-layer versus multilayer graphene. This is a potentially interesting topic which certainly deserves a thorough analysis. In the next sections we discuss and critically present the major results and propose additional studies that could be used in the context of assessing the safety of GFNs. The current studies are not exhaustive nor do they cover all aspects associated with the impact of graphenes on health. Most of the available studies have used GO and rGO. This focus on GO and rGO is likely related to their better solubility/dispersibility in water and physiological conditions in comparison to the other GFNs. The parameters that have been considered in these studies

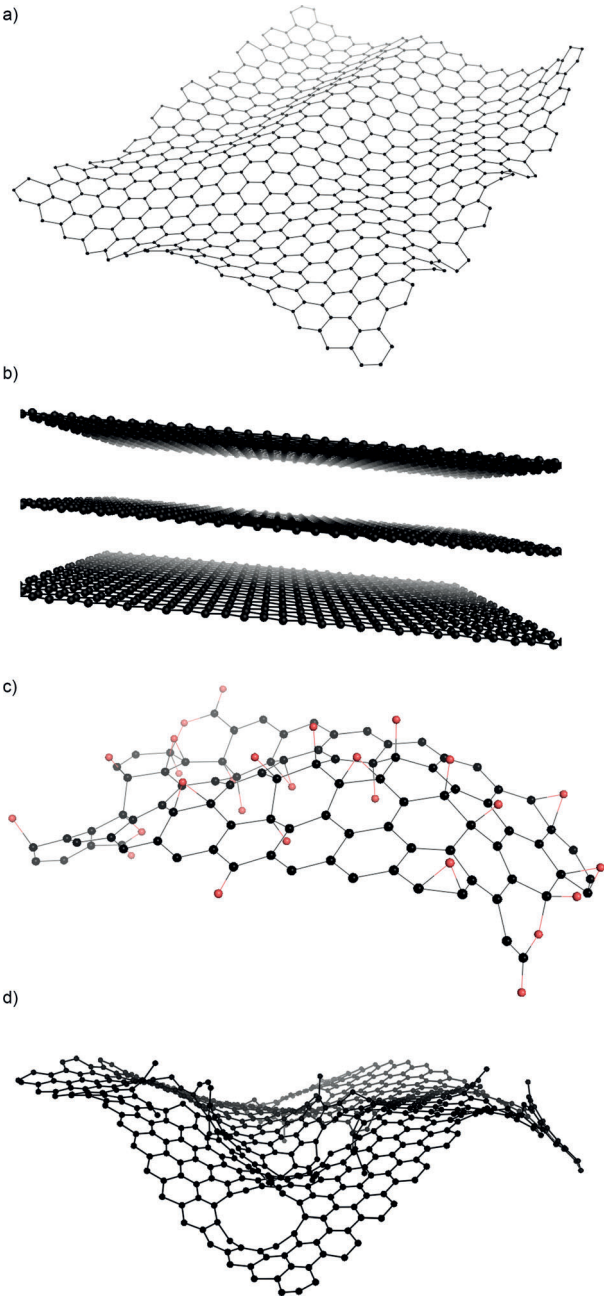

Figure 1. Representative chemical structures of some of the members of GFNs: a) graphene, b) few-layer graphene, c) graphene oxide (oxygen atoms are in red) and d) reduced graphene oxide.

Alberto Bianco received his Ph.D. in 1995 from the University of Padova. He was a visiting scientist at the University of Lausanne (1992), University of Tübingen (1996–1997), and University of Padova (1997–1998). In 2012, he received a fellowship invitation from JSPS for research in Japan. He is currently the Research Director at the CNRS in Strasbourg. His research interests focus on the functionalization of carbon-based nanomaterials for therapeutic, diagnostic, and imaging applications, and their impact on health and the environment.

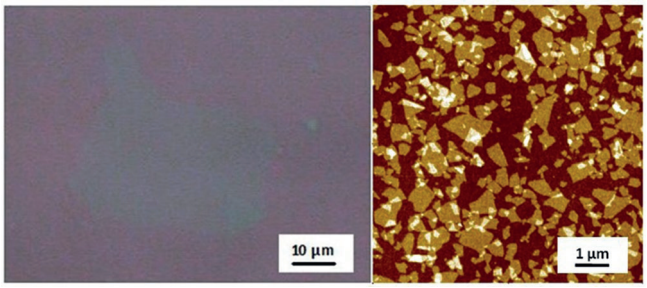

Figure 2. Optical (left) and AFM (right) images of graphene oxide spin coated onto a surface of silicon oxide (Courtesy of Vincenzo Palermo and Emanuele Treossi).

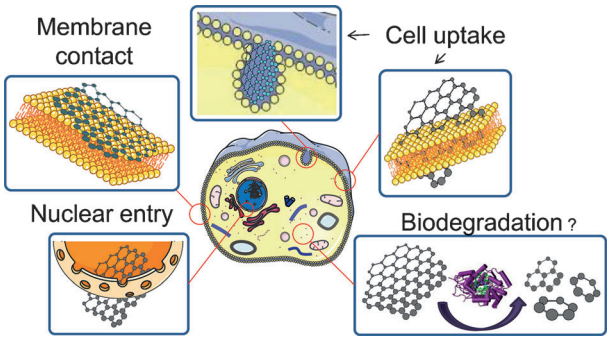

Figure 3. Possible interactions of GFNs at the plasma membrane level, during cell uptake at the nuclear membrane, and in the cytoplasm where degradation may occur.

comprise the type and quality of material (the presence of impurities might give false positive results), the type of cells, the doses (concentration range goes from 0.01 to 1000 $\mu g\,mL^{-1}$), the times of incubation and, in the case of animal experiments, the routes of administration. In most cases, the tested doses which can be associated to a potential danger are higher than the concentrations of nanomaterials generally used for therapeutic, imaging, or diagnostic purposes.

3. In vitro Effects of GFNs

In all studies related to new materials and their impact on living systems, the first screening is generally performed at the cellular level, thus leading to the in vitro assessment of potential cytotoxic effects. What happens to GFNs when in contact with cells? It can be anticipated that if they have the correct dimensions they can be internalized by different mechanisms (see below). Once inside the cells this material might then escape from subcellular compartments, travel within the cytoplasm, and translocate into the nucleus (Figure 3). In addition, GFNs might eventually undergo an oxidative degradation. Besides their mechanical behavior, GFNs can display a certain degree of cytotoxicity. The following examples illustrate the biological effects of GFNs, and the possible mechanisms leading to undesired effects.

In an initial comparative study, graphene and single-walled carbon nanotubes were tested on rat neuronal PC12 cells at concentrations ranging from 0.1 to 100 $\mu g\,mL^{-1}$ (Table 1).[21] Both materials showed a dose-dependent cytotoxicity. At low concentration ($<1\,\mu g\,mL^{-1}$) graphene induced a stronger metabolic activity than single-walled nanotubes. This behavior was reversed at the higher concentrations. High oxidative stress was also measured for graphene, with reactive oxygen species generated in a concentration- and time-dependent manner. Caspase-3 activation was indicative of the beginning of an apoptotic process. The effects evidenced by comparing the behavior of graphene versus carbon nanotubes indicate that the shape of the material plays a primary role. This study has assessed a cytotoxicity profile of graphene in terms of oxidative potential depending on cell exposure doses. In another study, GO (inappropriately called pristine graphene) and carboxylated GO (GO which underwent a mild acid treatment to add more COOH groups) were tested on monkey renal cells at concentrations between 10 and 300 $\mu g\,mL^{-1}$.[22] While GO accumulated mainly at the cell membrane, thus provoking significant destabilization of the F-actin alignment, more of the hydrophilic carboxylated GO was internalized by the cells and accumulated in the perinuclear region without affecting the cytoskeletal morphology, even up to the maximum dose tested (300 $\mu g\,mL^{-1}$). No physical damage of the cell membrane leading to necrosis was observed for either of the nanomaterials, thus supporting the hypothesis that another mechanism of cell death, likely involving intracellular stress triggering programmed cell death, was contributing to cytotoxicity. Particular attention is required regarding the definition of the material presented in these latter studies as pristine graphene corresponded instead to GO, and this might create certain confusion when the cytotoxic behavior of the materials is compared. F-actin filament localization of GO, modified with polyethylene glycol amine, has been also very recently reported.[23] Cell-cycle alterations, apoptosis, and oxidative stress were observed at a 75 $\mu g\,mL^{-1}$ concentration. Other similar studies have shown that cytotoxicity of GO and oxidized graphene nanoribbons (tested in the range 10–400 $\mu g\,mL^{-1}$) can be also strongly dependent on the type of cells and the cell culture conditions.[24–26]

In relation to the discovery of the antibacterial activity of GO (see section on Bacterial toxicity) and the possibility to exploit this property to treat eye related diseases, an interesting study reported the results on intraocular biocompatibility of such materials.[27] The influence of GO on morphology, viability, membrane integrity, and apoptosis was studied on human retinal pigment epithelial cells. Changes in cell viability and morphology were observed only after long culture times.

To extend the studies on the effects of GO in terms of cell viability and cellular responses, layers having different lateral sizes (i.e., 350 nm and 2 μm) were tested. Within six different cell lines cultured with GO, only the two phagocytic cell lines were able to internalize both nano- and microsized GO.[28] In terms of cell viability, little difference was observed for up to 20 $\mu g\,mL^{-1}$ of GO (the maximum tested dose). The presence

of manganese within the samples as a contaminant, derived from a non-accurate purification during the oxidative process to prepare GO, induced instead a general high cell mortality. This result hihglights the importance of the purification steps so as to avoid false positives which might be erroneously associated with an undesired effect of the tested nanomaterial. The uptake by macrophages was studied in a concentration range between 2 and 6 $\mu g\,mL^{-1}$. Cellular internalization kinetics showed that GO of 350 nm and GO of 2 μm had an identical intracellular accumulation after 24 hours. To clarify the size-independent uptake, the mechanisms of cell penetration were analyzed. This analysis clearly showed that the two GOs had different initial cell interaction processes (i.e. the 350 nm GO was wrapped by the active filopodia of macrophages while 2 μm GO entered the cell membrane nearly perpendicularly) and the intracellular localization was dictated by their size, thus leading to different compartmentalizations. Once inside the cells, the bigger 2 μm GO formed wrinkles and tended to fold with sequestration into lysosomes to some extent. After internalization it was observed that the bigger GO flakes induced a much stronger inflammatory response with high release of key cytokines. These results are extremely interesting as the different behaviors of the two types of GOs can be exploited in alternative biomedical contexts. The unexpected up-regulation of the cytokines by microsized GO can be used, for example, as an adjuvant effect in vaccine systems to activate weak immune responses. Low inflammatory profiles exerted by nanosized GO can be beneficial for applications in cancer therapy, where improved biocompatibility is demanded. In a similar study, C2C12 (mouse mesenchymal progenitor) cells were treated with protein-coated (with bovine serum albumin) GO of different sizes to elucidate the uptake mechanisms.[29] GO with a lateral dimension of about 500 nm was internalized by clathrin-mediated endocytosis, whereas larger sheets (about 1 μm) underwent a phagocytosis uptake. Very little inhibition of cell proliferation was observed for both types of graphenes up to 100 $\mu g\,mL^{-1}$. Figure 4 illustrates an example of GO uptake by murine peritoneal macrophages as performed in our laboratory.

The study on macrophages was also extended to pristine graphene dispersed in 1 % pluronic F108.[30] Murine macrophages, treated with graphene at a concentration between 20 and 100 $\mu g\,mL^{-1}$, underwent a dose-dependent apoptosis through a mechanism involving a decrease of mitochondrial potential and an increase of reactive oxygen species (ROS). The identification of different mechanisms that trigger macrophage apoptosis is extremely useful and provides important information for developing possible strategies to control programmed cell death induced by graphene. Murine macrophages incubated with GO (maximum dose of 100 $\mu g\,mL^{-1}$) were also able to elicit autophagy and Toll-like receptor associated inflammatory responses.[31] Interestingly, autophagy is exploited by cells to eliminate endogenous molecules, thus suggesting one possible way used by cells to clear internalized graphene-based nanomaterials. Besides macrophages, dendritic cells (DCs) are another class of key immune cells. DCs are important because they induce and maintain T-cell-mediated immunity and immune tolerance.

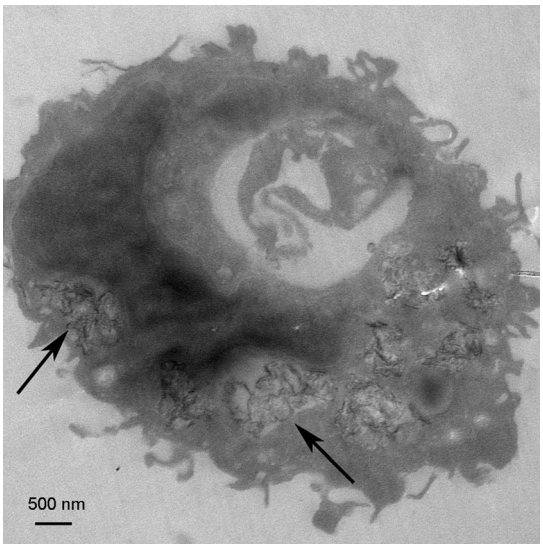

Figure 4. GO is internalized by murine peritoneal macrophages. The arrows indicate the presence of GO sheets into the phagosomes.

DCs treated with GO (in the concentration range 1–25 $\mu g\,mL^{-1}$) were affected in their functional activity.[32] DC antigen presentation was inhibited by GO. This alteration was associated to a down-regulation of the intracellular levels of one unit of the immunoproteasome responsible for antigen processing in DCs. This study underlines the importance of carefully assessing the immunomodulatory effects of new nanomaterials.

Along with the development of graphene and the other family members as delivery systems for systemic administration of therapeutic molecules,[8,9] it is important to evaluate the haemocompatibility as the material encounters blood components.[33,34] In the comparison between graphene and GO, the former showed a slightly higher cytotoxic effect as a result of the strong hydrophobic interaction with cell membranes. However, both graphenes showed little haemolysis of red blood cells (in the range 10–75 $\mu g\,mL^{-1}$ concentration).[33] Graphene did not influence the coagulation pathways, thus suggesting a low risk of thrombosis once intravenously administered. Although it is difficult to compare the tested materials, the previous results are clearly in contrast to those of two studies which proved the thrombotoxicity potential of GO.[34–36] GO was demonstrated to have a significant haemolytic activity and be highly thrombogenic, thus inducing strong aggregation of human platelets (at 2 $\mu g\,mL^{-1}$). To modulate the cytotoxicity, GO was either coated with chitosan[34] or its carboxylic functions were either reduced by thermal annealing[34,35] or transformed into ammonium groups by Curtius rearrangement.[36] The second transformation led to a new functionalized material with no effect on stimulation of platelets, no lysis of erythrocytes, and the absence of thromboembolysis induction. What still remains unclear is what really happens during the chemical transformation of the carboxylic groups into amines as graphene oxide also contains hydroxy groups, epoxides, ketones, and aldehydes which should not undergo Curtius rearrangement. These studies illustrate how the toxic effects

of GO on red blood cells can be alleviated by chemical modification of the material.

Complementary tests to assess the impact of carbon nanomaterials on cells consisted of the analysis of the possible changes on the protein profile.[37,38] rGO (inappropriately called graphene as obtained by hydrazine treatment of GO) and single-walled carbon nanotubes were compared for the expression of proteins involved in the metabolic pathway, redox regulation, cytoskeleton formation, and cell growth. While carbon nanotubes severely interfere with the expression of a series of these proteins, only moderate variation of the protein levels was observed on human hepatoma cells treated with rGO. This data indicates that reduced graphene oxide is less cytotoxic than carbon nanotubes in terms of possible alterations of the protein function. GO, free or dispersed with surfactants, was also tested on human and murine fibroblasts.[39,40] Dose-dependent toxicity on cells was observed (i.e., 3–100 $\mu g\,mL^{-1}$ concentration). An opposite result was reported in two independent studies showing that GO induced only a slight decrease on proliferation of the A549 cell line without signs of apoptosis or cell death in a range of concentrations between 7.8 and 200 $\mu g\,mL^{-1}$.[41–43] The same material, treated with hydrazine to generate rGO, resulted instead in high cytotoxicity, thus significantly lowering the viability of the same type of cells.[41]

An alternative to the reduction with hydrazine, other chemical approaches can be used to modify GO. Covalent PEGylation (PEG = polyethylene glycol) or functionalization with biocompatible polymers (i.e., dextran) modulates the cytotoxic effect on a series of cell lines, thus leading to an increased cell viability up to a dose of 200 $\mu g\,mL^{-1}$.[6,44,45] PEG-GO, with a less than 50 nm side edge, was stable under physiological conditions and penetrated the cells, most likely through an endocytosis mechanism, and displayed no evident toxicity at the various concentrations.[6]

The current results can be considered important initial data which have been gathered on the in vitro toxicity of GFNs. However, to avoid a situation similar to carbon nanotubes, it is important to not generalize but rather take into consideration the great variability of the materials. It is essential to compare the different types of GFNs and correlate their impact on cells to their physicochemical characteristics and, in some case, to the chemical modifications introduced. This approach will avoid generalization and the description of all types of graphenes as being eventually dangerous for human health when it is in fact not the case for some of them.

4. In vivo Effects of GFNs

The assessment of the in vivo toxic effects of GFNs in animal models has also been investigated, albeit to a lesser extent (Table 2). GO and rGO were used to analyze the effect on blood platelets, the cells responsible for the maintenance of homeostasis and thrombus formation.[35,36] GO elicited a strong aggregatory response in platelets, whereas intravenous administration in mice induced extensive pulmonary thromboembolism. This behavior was associated with the charge distribution on the surface of GO as the aggregation properties were significantly lowered when the material was chemically treated to generate rGO. In vivo toxicity of GO was evaluated in mice and rats after intravenous administration.[39,46] Significant pathological changes including inflammatory cell infiltration, pulmonary aedema, and formation of granulomas were found using a dose of 10 $mg\,kg^{-1}$ body weight. In contrast, GO showed good biocompatibility with red blood cells at very low doses while haemolysis was induced at 80 $\mu g\,mL^{-1}$.

Pulmonary toxicity is a major concern in case of the industrial production of nanomaterials, as their respirability might cause damage and eventually long-term diseases in humans who come into contact with this type of material. It has been shown that GO and aggregated graphene provoked severe and persistent injury in the lungs after direct injection (i.e. 50 μg per animal) into the organs of mice.[47] But the toxic effects were clearly reduced in the case of pristine graphene dispersed in pluronic surfactant. Apparently the oxidation of graphene is the cause of pulmonary toxicity. In another recent study, the risk to the respiratory system was also demonstrated for pristine graphene nanoplatelets which were constituted of few-layer graphene, up to 25 μm in size, dispersed in 0.5 % bovine serum albumin.[20] Graphene nanoplatelets were found to deposit beyond the ciliated airways after inhalation (i.e., 50 μg of nanoplatelets per animal). Acute inflammatory responses in mice, cell inflammation, and frustrated macrophage phagocytosis were evidenced. The inflammogenicity in vitro and in vivo was attributed to the respirable aerodynamic diameter, the index that determines the respirability of a particle and the site of deposition. Eventually, the deposition in the lung could originate, in long-term mesothelioma or other pleural pathological conditions. It is difficult to understand what the differences in these two studies are and how they account for the opposite behavior of pristine graphene. It is likely that the morphology of the tested materials, the number of layers, the surface area, and the dispersion procedures are among the parameters which can give rise to the different toxicity properties. It is not surprising that materials at the micrometer size display a worrying degree of toxicity.[48,49] In contrast, the presence of contaminants as unreacted graphite oxide or graphitic fractions might be also responsible for inflammation. Indeed, when GO is extensively purified using several washings and centrifugation steps it did not show an increase in the level of proteins and polymorphonuclear leukocytes on days 1 and 7 after peritoneal administration (injected dose of 50 μg per animal).[43] No collection of giant cells, inflammatory response, and formation of granuloma were evidenced in comparison to long pristine multiwalled carbon nanotubes (Figure 5). As the model used to assess the carcinogenic potential after the exposure to GO was designed for fiber-shaped materials,[49] it is still not clear if the same model is appropriate for nanomaterials with alternative shapes.

The modulation of toxicity in vivo can be achieved through chemical functionalization.[50] PEGylation of GO reduces, for example, the toxic effect in mice. In looking at the use of GO as a component of injectable hydrogels for tissue engineering, no severe toxicity was measured in vivo.[51] What

Table 1: Different GFNs used for in vitro studies and their biological effects.

Material	In vitro model	Tested dose	Biological effects	Ref.
Graphene	Neuronal PC12 cells	0.01–100 $\mu g\,mL^{-1}$	Increase of activation of caspase-3; Low release of LDH; High generation of ROS	[21]
Pristine graphene (GO)	Monkey renal cells (Vero)	10–300 $\mu g\,mL^{-1}$	Cell membrane accumulation; F-actin destabilization; Dose-dependent oxidative stress; Cell death at 50 $\mu g\,mL^{-1}$	[22]
Carboxylated GO	Monkey renal cells (Vero)	10–300 $\mu g\,mL^{-1}$	Cell uptake; No LDH leakage; No cell death or apoptosis up to 300 $\mu g\,mL^{-1}$	[22]
GO decorated with polyethylene glycol-amine	Saos-2 osteoblasts; MC3T3-E1 preosteoblasts; Murine RAW 264.7 macrophages	75 $\mu g\,mL^{-1}$	F-actin localization; Cell-cycle alteration; Apoptosis; Oxidative stress	[23]
GO	Neuroblastoma SH-SY5Y cells	10–100 $\mu g\,mL^{-1}$	Dose and time dependent effect on cell viability above 80 $\mu g\,mL^{-1}$; Enhanced differentiation induced by retinoic acid	[24]
GO	Normal human lung cells (BEAS-2B)	10–100 $\mu g\,mL^{-1}$	Concentration- and time-dependent apoptosis	[25]
Oxidized graphene nanoribbons coated with PEG-DSPE	HeLa cells; NIH 3T3 cells; SKBR3 cells; MCF-7cells	10–400 $\mu g\,mL^{-1}$	Dose-dependent and time-dependent decrease of viability; Cell-specific cytotoxicity; Significantly higher cytotoxicity for HeLa cells (at 10 $\mu g\,mL^{-1}$) as a consequence of a higher uptake by these cells in comparison to the other cells	[26]
GO	Human retinal pigment epithelium cells	5–100 $\mu g\,mL^{-1}$	Little influence on cell morphology: No significant apoptosis; Low release of LDH	[27]
GO (350 nm and 2 μm lateral size)	Human hepatocarcinoma cells (HepG2); Human breast MCF-7 cancer cells; Human umbilical vein endothelial cells (HUVEC); Lewis lung carcinoma cells (LLC); J774A.1 murine macrophages; PMØ peritoneal macrophages	1–20 $\mu g\,mL^{-1}$	No cell uptake by non-phagocytic cells; No size-dependent internalization in macrophages; No differences on cell viability up to 20 $\mu g\,mL^{-1}$; Strong inflammatory response by 2 μm GO; High release of cytokines by 2 μm GO	[28]
BSA-coated GO (420 nm and 860 nm lateral size)	C2C12 (mouse mesenchymal progenitor) cells	10–100 $\mu g\,mL^{-1}$	Different uptake mechanisms; No alteration of metabolic activity	[29]
Pristine graphene in 1% pluronic F108	Murine RAW 264.7 macrophages	20–100 $\mu g\,mL^{-1}$	Apoptosis through depletion of mitochondrial potential and increase of ROS; Different signaling pathways activated; Liberation of pro-apoptotic cytokines	[30]
GO	Murine RAW 264.7 macrophages	5 and 100 $\mu g\,mL^{-1}$	Induction of autophagy; Activation of TLR4 and TLR9; Cytokine secretion (IL2, IL10, INFγ and TNFα)	[31]
GO	Bone-marrow-derived dendritic cells (DCs)	1–25 $\mu g\,mL^{-1}$	No alteration of antigen engulfment; No effect on MHC-I/peptide–TCR interaction; Downregulation of the level of the subunit LMP7 of immunoproteasome	[32]
Graphene and GO	Red blood cells (RBCs)	10–75 $\mu g\,mL^{-1}$	No haemolysis up to 75 $\mu g\,mL^{-1}$; No platelet activation or aggregation; No risk of thrombosis	[33]
GO	Human erythrocytes (RBCs)	3.125–200 $\mu g\,mL^{-1}$	High haemolytic activity	[34]
Chitosan-coated GO	Human erythrocytes (RBCs)	100 $\mu g\,mL^{-1}$	No haemolytic activity	[34]
GO	Erythrocytes (RBCs)	5–25 $\mu g\,mL^{-1}$	Thrombotoxicity; Human platelet aggregation	[35]

Table 1: (Continued)

Material	In vitro model	Tested dose	Biological effects	Ref.
rGO	Erythrocytes (RBCs)	2–20 $\mu g\,mL^{-1}$	Reduced platelet aggregation	[35, 36]
Amino-GO	Erythrocytes (RBCs)	2–20 $\mu g\,mL^{-1}$	No thrombohaemolysis; No platelet stimulation; No cell lysis	[36]
rGO	Human hepatocarcinoma cells (HepG2)	1 $\mu g\,mL^{-1}$	Moderate variation of protein levels	[37, 38]
GO	Human fibroblasts (HDF)	5–100 $\mu g\,mL^{-1}$	Toxicity at doses $>50\ \mu g\,mL^{-1}$; Decrease of cell adhesion; Cell apoptosis	[39]
GO dispersed using PEG	L929 fibroblasts	3.125–100 $\mu g\,mL^{-1}$	Low toxicity up to 25 $\mu g\,mL^{-1}$	[40]
GO	A549 cells	20 and 85 $\mu g\,mL^{-1}$	Slight decrease on cell proliferation; No apoptosis or cell death up to 85 $\mu g\,mL^{-1}$	[41]
rGO	A549 cells	20 and 85 $\mu g\,mL^{-1}$	Remarkable reduction of cell viability	[41]
GO	A549 cells	10–200 $\mu g\,mL^{-1}$	No cell uptake; Dose-dependent oxidative stress; Slight loss of cell viability at 200 $\mu g\,mL^{-1}$	[42]
Purified GO	A549 cells	7.8–125 $\mu g\,mL^{-1}$	Dose-dependent cytotoxicity; 80% cell viability at 125 $\mu g\,mL^{-1}$	[43]
PEG-GO	RAJI cells; HCT-116 cells; OVCAR-3 cells; U87MG cells; MDA-MB-435 cells; MCF-7cells	0.5–150 $\mu g\,mL^{-1}$	No effect on cell viability up to 100 $\mu g\,mL^{-1}$; Reduced toxicity	[6, 44]
Dextran-GO	HeLa cells	10, 50, and 200 $\mu g\,mL^{-1}$	Enhanced cell viability; Normal cell proliferation	[45]
GO	NIH 3T3 cells	1000 $\mu g\,mL^{-1}$	No effect on cell viability	[58a]

is not really clear from this study is the role of graphene within the material besides reducing the concentration of the surfactant necessary to form a thermosensitive hydrogel. The capacity of GO to absorb in the near-infrared region is one of the advantages of integrating such material in a composite for regenerative medicine, as it can improve, by controlled irradiation, the release of a drug eventually embedded into the hydrogel.

In vivo studies have been expanded to animal models other than rodents.[52] *Caenorhabditis elegans* is a free-living nematode which offers the advantages of a laboratory culture. *C. elegans* (treated with a 250 $\mu g\,mL^{-1}$ solution) has been used as host to assess the efficacy of graphite nanoplatelets, composed of 3 to 60 graphene layers with a lateral size of 1 to 10 μm, as antimicrobial agents after exposure to the pathogen *Pseudomonas aeruginosa*. The presence of this material inside the nematodes clearly reduced the number of infective cells, likely a result of mechanical damage of the bacterial membrane, but it did not alter the organisms longevity and reproductive capacity (i.e., no genotoxicity). *C. elegans* has also been used in recent attempts to elucidate the chemical processes besides the toxicity of GO in vivo.[53] GO was coated with PEGylated poly-L-lysine or used uncoated. No changes in mean longevity, damage at the cell-wall level, impairment of locomotion, and reproducibility reduction of the nematode were observed when the organism was treated with GO in the concentration range of between 5 and 20 $\mu g\,mL^{-1}$. Instead, the polymer-coated GO significantly reduced the resistance of the nematode, particularly under oxidative or heat stress conditions, thus leading to death. The excessive presence of ROS impaired the inherent antioxidant defence system, thus provoking a dramatic toxic effect on *C. elegans* in pathophysiological conditions.

As for the in vitro impact, many parameters need to be taken into consideration when GFNs are tested for toxicity in vivo. Indeed, the variability of the samples is extremely high. Here the situation is similar to that observed for carbon nanotubes. Fundamentally, the morphological and physicochemical characteristics of each type of sample should be considered and described without making any generalizations, which can risk introducing a bias when statements on the safety or toxicity of GFNs are presented or emphasized. Toxicity of GFNs can be closely associated to their surface functionalization. The size is the second important parameter which needs to be carefully considered.

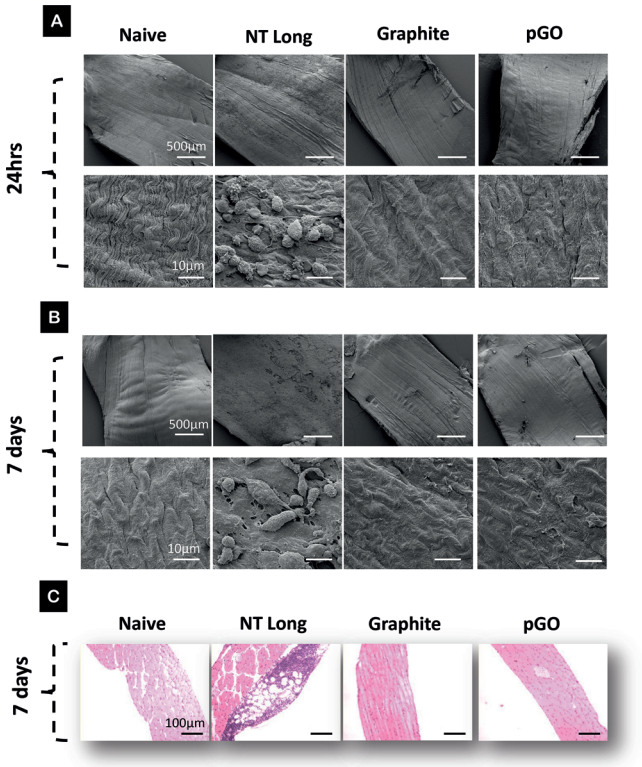

Figure 5. Granuloma formation on the diaphragm membrane after 7 days. Female C57Bl/6 mice were intraperitoneally injected with 50 μg of vehicle control (0.5% bovine serum albumin/saline), pristine multi-walled carbon nanotubes (NT long, pristine), and graphite and pure GO (pGO). The mice were killed after 1 day and 7 days and the diaphragms excised, fixed, and prepared for visualization. SEM images of the diaphragm surface (A-B), and the histology using hematoxylin and eosin staining (C), show the collection of giant cells and highlight the presence of granulomatous inflammation with NT long, but not with graphite and pGO. Low and high magnifications of the SEM images are shown. Reproduced with permission.[43] Copyright 2012, Wiley-VCH Verlag GmbH & Co.

5. Bacterial Toxicity of GFNs

Concerning the toxic effects of GFNs on microorganisms, there is a series of recent studies on different types of bacteria and fungi. The apparent antibacterial activity might find interesting future applications of graphene in antimicrobial products (Figure 6). GO and rGO, deposited on a stainless steel substrate, showed antimicrobial activity against gram-negative *E. coli* and gram-positive *S. Aureus*.[54] rGO was more efficient in inactivating both types of pathogens. The effect on the metabolic activity was combined with the damage of the microorganism cell membrane.[41] To further expand these studies, the antimicrobial mechanism was also analyzed by comparing different types of graphene materials, including graphite, graphite oxide, GO of different lateral sizes, and rGO (5–80 $\mu g\,mL^{-1}$ concentration; Figure 6).[55] Again, higher antibacterial activity was found for GO, which had the smallest average size among the different types of graphene derivatives.

The physicochemical characteristics of graphene materials seem to play an important role in the efficiency of the bacterial killing and therefore can be tailored to reduce the adverse impact on health and the environment. However, the results were questioned by another study,[56] wherein GO was added to *E. coli* and the bacteria grew faster by forming dense biofilms around the suspended nanomaterial. Only the combination with silver nanoparticles showed cell death.[56,57] In view of these findings, the exploration of the bacteriostatic properties of GO is challenging and will certainly stimulate further studies.

Graphite nanoplatelets and other types of GFNs have demonstrated bactericide properties in vitro on isolated *P. aeruginosa* and in vivo on a host nematode challenged with the same pathogen.[52] Antibacterial activity of GO was preserved or even improved when dispersed in poly-*N*-vinylcarbazole and electrodeposited on a substrate, without

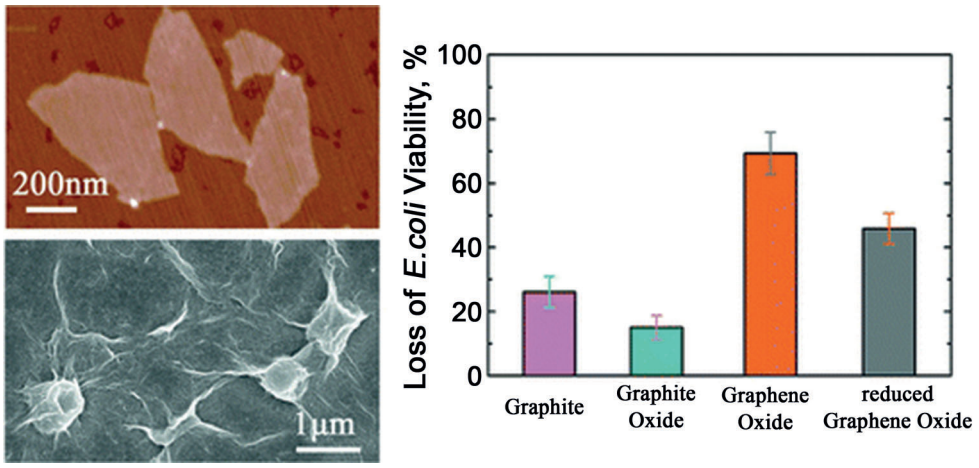

Figure 6. AFM image of GO sheets dried on a mica surface (top left). *E. coli* cells after incubation with GO dispersion (40 $\mu g\,mL^{-1}$) for 2 h; most of bacteria become flattened, and lose their cellular integrity after exposure to GO dispersions (bottom left). Cell viability measurement after incubation with graphite, graphite oxide, GO, and rGO dispersions (graph). A 5 mL portion of graphene-based materials (80 $\mu g\,mL^{-1}$) was incubated with *E. coli* for 2 h at 37 °C. Loss of cell viability was obtained by colony counting method. Isotonic saline solution without graphene-based materials was used as control. Reproduced with permission.[55a] Copyright 2011, American Chemical Society.

Table 2: Different GFNs used for in vivo studies and their biological effects.

Material	In vivo model	Tested dose	Biological effects	Ref.
GO	Rabbits	100–300 μg/eye	No eye changes: Normal intraocular pressure; Normal eyesight	[27]
GO	Mice	250 $\mu g\,kg^{-1}$	Thrombotoxicity; Extensive pulmonary thromboembolism; Human platelet aggregation	[35]
rGO	Mice	250 $\mu g\,kg^{-1}$	Less effective in platelet aggregation	[35, 36]
Amino-GO	Mice	250 $\mu g\,kg^{-1}$	Absence of thrombotoxicity; Vessels appear normal with no sign of occlusive pathology	[36]
GO	Mice	100, 250, and 400 μg/animal	Chronic toxicity and animal death at the highest dose; Lung, spleen and liver granulomas; No kidney clearance	[39]
Purified GO	Mice	50 μg/animal	Absence of acute and chronic inflammation after intraperitoneal administration	[43]
Dextran-GO	Mice	20 $mg\,kg^{-1}$	Accumulation in liver and spleen; Gradual clearance within one week; No short-term toxicity	[45]
GO	Mice/rats	1 and 10 $mg\,kg^{-1}$ (animals) 10 and 80 $\mu g\,mL^{-1}$ (cells)	Dose dependent pulmonary toxicity; Granulomatous lesions at 10 $mg\,kg^{-1}$; Pulmonary aedema fibrosis at 10 $mg\,kg^{-1}$; Inflammatory cell infiltration at 10 $mg\,kg^{-1}$; RBC haemolysis at 80 $\mu g\,mL^{-1}$	[46]
GO and aggregated graphene	Mice	50 μg/animal	Generation of ROS; Inflammation; Apoptosis; Increase of the rate of mitochondrial respiration; Pulmonary toxicity inflammation	[47]
Graphene in 2% pluronic F108	Mice	50 μg/animal	Reduced toxic effects	[47]
Graphene nanoplatelets (25 μm size) in 0.5% BSA	Rats	50 μg/animal (pharyngeal aspiration) 5 μg/animal (intrapleural injection)	Inflammatory cytokine release (IL1β); Acute pulmonary inflammatory response	[20]
PEG-GO	Mice	20 $mg\,kg^{-1}$	High tumor accumulation; Low uptake by RES; No sign of abnormality on kidney, spleen, heart, liver and lung; Gradual elimination	[50]
GO-pluronic hydrogels	Mice	Gel composition: 0.4% GO-0.25–1% pluronic	No severe toxicity	[51]
Graphite nanoplatelets (1–tens μm)	*Caenorhabditis elegans*	50–250 $\mu g\,mL^{-1}$	No alteration of nematode longevity; No alteration of reproductive capacity	[52]
GO and PEG–(poly-L-lysine)-coated GO	*Caenorhabditis elegans*	5–20 $\mu g\,mL^{-1}$	No alteration of nematode longevity; No damage at the level of cell walls; No alteration on reproductive capacity; No reduction of locomotion	[53]
PEG–(poly-L-lysine)-coated GO	*Caenorhabditis elegans*	5–20 $\mu g\,mL^{-1}$	Cells are cultured under oxidative or heat stress: Reduced resistance leading to death; Intracellular ROS formation; Impaired electron transfer process	[53]
PEG-GO	Mice	20 $mg\,kg^{-1}$	RES accumulation; Renal and faecal elimination; No alteration of biochemical blood parameters	[61]
GO (large 1–5 μm and small 110–500 nm)	Mice	1–10 $mg\,kg^{-1}$	Quick elimination from blood; Accumulation mainly in lung and liver	[62]

cytotoxic effects on mammalian cells exposed to a dose of 1000 $\mu g\,mL^{-1}$.[58] Interestingly, the interaction of GO with *E. coli* led to a reduction of the graphene sheets (loss of 60% of oxygen-containing functional groups) drop-casted on a Si_2O/Si(100) substrate.[59] During this process the bacteria showed an inhibition of the proliferation and a surface detachment,

thus accounting for an antibacterial activity of rGO generated by the bacterial metabolic action. rGO (tested between 1 and 500 $\mu g\,mL^{-1}$) also displayed antifungal activity on the nonpathogenic *Aspergillus oryzae* and on the pathogenic *Aspergillus niger* and *Fusarium oxysporum*.[60] While this property can be useful for pathogenic fungi, a certain concern needs to be considered in the case of toxic effects on nonpathogenic microorganisms important for the metabolism or the environment.

The comparison between the available data on antibacterial and antifungal activity of GFNs is difficult because the conditions of cell culture and the type of starting materials differ within the reported experiments. In contrast, some of the conflicting data can stimulate the research towards the assessment of the antimicrobial role of GFNs as a function of their physicochemical properties.

6. Biodistibution and Pharmacokinetics of GFNs

The in vivo study of the biodistribution, accumulation, and elimination of graphene nanomaterials is a fundamental step to understanding the risks associated with their uses. Biodistribution studies (injected doses of 1 or 10 $mg\,kg^{-1}$) have shown that intravenously injected GO accumulates predominantly in the lungs, and low uptake by the reticuloendothelial system (RES) was observed (Table 2).[46] GO exhibited a long circulation time in comparison to other carbon forms. No pathological modifications in different organs were evidenced after injection of 1 $mg\,kg^{-1}$ body weight, but significant changes were evidenced in the lung at a dose of 10 $mg\,kg^{-1}$. Interestingly, PEG-GO accumulates mainly in the tumor of xenografted animals with a lower uptake than that by the RES, and there are no significant toxic effects.[50] Following an initial accumulation in RES organs, a gradual elimination was observed between 3 and 15 days. After three months the graphene sheets were completely eliminated without signs of abnormality in major organs (i.e., kidney, liver, spleen, heart and lung). This type of modified graphene radiolabeled with ^{125}I was also used to evaluate more thoroughly the pharmacokinetics, the long-term biodistribution, and the toxic effects.[61] The intravenously administered graphene sheets were gradually cleared by both renal and faecal elimination. The tested dose of 20 $mg\,kg^{-1}$ did not provoke evident toxicity within a 3 month period, as proved by measuring the biochemical parameters in blood, and the haematological markers (white and red blood cells, haemoglobin, platelets, etc.). Histological examination of the different organs did not show evidence of damage or lesions, but an increase of color of the spleen and liver resulting from accumulation of brown GO was observed. The impact of the lateral size of GO sheets on organ distribution and accumulation was also assessed with iodinated material.[62] Large GO (1–5 μm) and small GO (110–500 nm) were labeled with $Na^{125}I$. Regardless the size, GO was eliminated quickly from the blood and accumulated mainly in the lung and liver. While small GO was found in the liver, large GO accumulated in the lungs. As the doses of injected small GO increased from 1 to 10 $mg\,kg^{-1}$, its distribution changed, thus showing higher localization in the lungs as a consequence of the aggregation occurring at high concentrations. The comparison between the pharmacokinetic profile of the two types of GO suggests that a material with a small lateral dimension is more suitable for potential biomedical applications.[43]

The data of these studies are extremely interesting and they will encourage additional investigations. It is indeed necessary to compare the behavior of other graphene nanomaterials, other animal models, higher doses, and alternative routes of administration. These studies will allow an understanding of the effects of GFNs either administered on purpose or brought into by accidental exposure, in order to facilitate their development for use in materials science and biomedicine.

7. Summary and Outlook

This Minireview summarizes the different case studies on the in vitro and in vivo impact of GFNs. Are therefore GFNs safe or toxic? The results available show that this new nanomaterial might become a health hazard, but chemical manipulation can alleviate the potential risks associated with the future development of GFNs for different applications (i.e., composites, electronic devised biomedical tools, etc.). Along these lines, very recently a comparison between GFNs and carbon nanotubes appeared, thus giving some guidelines about how to modulate the toxic effects of graphenes.[13] If we consider such rules, we might avoid to accumulate retard in addressing the problem as it has been done for carbon nanotubes. In this context, this Minireview can be also considered anticipatory and it is aimed at drawing the attention of the researcher towards developing new nanomaterials. It is not possible to give a clear answer to the initial question, but there is strong evidence that the toxic effects are modular. In addition, a generalization on the toxicity of GFNs should be avoided as the risks associated with these new nanomaterials are dependent on the specific applications and development.

Future research is however necessary to thoroughly explore the biological responses and the safety issues of GFNs by taking into consideration the different physicochemical properties. The more studied GO and rGO are more hydrophilic than single- and multilayer graphene. The difficulty in maintaining stable colloidal dispersions of hydrophobic graphene surfaces is one of the limitations on the evaluation of the safety profile of this nanomaterial. However, the analyses should be clearly expanded to all members of the graphene family (i.e., graphene dots).[63]

There are several key factors associated with the toxicity of new nanomaterials. The generation of oxygen reactive species, the indirect toxicity because of GFN adsorption of important biomolecules, and physical toxicity associated with the interaction with the lipids constituting cell membranes, tissues, and organs need to be carefully studied and analyzed. In addition, study of the uptake as a function of the dimension is necessary. Side dimensions of graphene might affect the different receptors responsible of the energy-dependent mechanisms of cell penetration (i.e., endocytosis/phagocyto-

sis active mechanisms). If passive mechanisms, as in the case of carbon nanotubes,[64] are taking place, it is interesting to understand how the flat form of the material affects the membrane organization (i.e., membrane disruption or simple sliding between the lipid bilayers).[65] All these studies will help formulate a safer design, production, and manufacturing of GFNs to minimize the risks for human health and the environment.

The author wishes to thank the Centre National de la Recherche Scientifique (CNRS) and the Agence Nationale de la Recherche (DECANO, project no. ANR-2011-CESA-007-01). The author wishes to thank Fanny Bonachera for her help on the preparation of the figures, and Hélène Dumortier and Cécilia Ménard-Moyon for critical reading of the manuscript.

Received: November 13, 2012
Revised: December 13, 2012
Published online: April 11, 2013

[1] K. S. Novoselov, A. K. Geim, S. V. Morozov, D. Jiang, Y. Zhang, S. V. Dubonos, I. V. Grigorieva, A. A. Firsov, *Science* **2004**, *306*, 666 – 669.
[2] a) X. Huang, Z. Yin, S. Wu, X. Qi, Q. He, Q. Zhang, Q. Yan, F. Boey, H. Zhang, *Small* **2011**, *7*, 1876 – 1902; b) X. Huang, X. Qi, F. Boey, H. Zhang, *Chem. Soc. Rev.* **2012**, *41*, 666 – 686.
[3] K. P. Loh, Q. Bao, G. Eda, M. Chhowalla, *Nat. Chem.* **2010**, *2*, 1015 – 1024.
[4] Y. Cui, S. N. Kim, R. R. Naik, M. C. McAlpine, *Acc. Chem. Res.* **2012**, *45*, 696 – 704.
[5] C. Li, J. Adamcik, R. Mezzenga, *Nat. Nanotechnol.* **2012**, *7*, 421 – 427.
[6] Z. Liu, J. T. Robinson, X. M. Sun, H. J. Dai, *J. Am. Chem. Soc.* **2008**, *130*, 10876 – 10877.
[7] K. S. Novoselov, V. I. Fal'ko, L. Colombo, P. R. Gellert, M. G. Schwab, K. Kim, *Nature* **2012**, *490*, 192 – 200.
[8] Y. Zhang, T. R. Nayak, H. Hong, W. Cai, *Nanoscale* **2012**, *4*, 3833 – 3842.
[9] a) H. Shen, L. Zhang, M. Liu, Z. Zhang, *Theranostics* **2012**, *2*, 283 – 294; b) K. Yang, Y. Li, X. Tan, R. Peng, Z. Liu, *Small* **2013**, DOI: 10.1002/smll.201201417; c) K. Yang, L. Feng, X. Shi, Z. Liu, *Chem. Soc. Rev.* **2013**, *42*, 530 – 547.
[10] L. Feng, Z. Liu, *Nanomedicine* **2011**, *6*, 317 – 324.
[11] V. C. Sanchez, A. Jachak, R. H. Hurt, A. B. Kane, *Chem. Res. Toxicol.* **2012**, *25*, 15 – 34.
[12] L. Yan, F. Zhao, S. Li, Z. Hu, Y. Zhao, *Nanoscale* **2011**, *3*, 362 – 382.
[13] C. Bussy, H. Ali-Boucetta, K. Kostarelos, *Acc. Chem. Res.* **2013**, *46*, 692 – 701.
[14] A. M. Jastrzębska, P. Kurtycz, A. R. Olszyna, *J. Nanopart. Res.* **2012**, *14*, 1320 – 1328.
[15] K. Kostarelos, A. Bianco, M. Prato, *Nat. Nanotechnol.* **2009**, *4*, 627 – 633.
[16] G. P. Kotchey, B. L. Allen, H. Vedala, N. Yanamala, A. A. Kapralov, Y. Y. Tyurina, J. Klein-Seetharaman, V. E. Kagan, A. Star, *ACS Nano* **2011**, *5*, 2098 – 2108.
[17] a) W. S. Hummers Jr., R. E. Offeman, *J. Am. Chem. Soc.* **1958**, *80*, 1339 – 1339; b) L. J. Cote, R. Cruz-Silva, J. Huang, *J. Am. Chem. Soc.* **2009**, *131*, 11027 – 11032.
[18] A. Dimiev, D. V. Kosynkin, L. B. Alemany, P. Chaguine, J. M. Tour, *J. Am. Chem. Soc.* **2012**, *134*, 2815 – 2822.
[19] K. P. Loh, Q. Bao, P. K. Ang, J. Yang, *J. Mater. Chem.* **2010**, *20*, 2277 – 2289.
[20] A. Schinwald, F. A. Murphy, A. Jones, W. MacNee, K. Donaldson, *ACS Nano* **2012**, *6*, 736 – 746.
[21] Y. Zhang, S. F. Ali, E. Dervishi, Y. Xu, Z. Li, D. Casciano, A. S. Biris, *ACS Nano* **2010**, *4*, 3181 – 3186.
[22] A. Sasidharan, L. S. Panchakarla, P. Chandran, D. Menon, S. Nair, C. N. Rao, M. Koyakutty, *Nanoscale* **2011**, *3*, 2461 – 2464.
[23] M.-C. Matesanz, M. Vila, M.-J. Feito, J. Linares, G. Gonçalves, M. Vallet-Regi, P.-A. A. P. Marques, M.-T. Portolés, *Biomaterials* **2013**, *34*, 1562 – 1569.
[24] M. Lv, Y. Zhang, L. Liang, M. Wei, W. Hu, X. Li, Q. Huang, *Nanoscale* **2012**, *4*, 3861 – 3866.
[25] N. V. Vallabani, S. Mittal, R. K. Shukla, A. K. Pandey, S. R. Dhakate, R. Pasricha, A. Dhawan, *J. Biomed. Nanotechnol.* **2011**, *7*, 106 – 107.
[26] S. M. Chowdhury, G. Lalwani, K. Zhang, J. Y. Yang, K. Neville, B. Sitharaman, *Biomaterials* **2013**, *34*, 283 – 293.
[27] L. Yan, Y. Wang, X. Xu, C. Zeng, J. Hou, M. Lin, J. Xu, F. Sun, X. Huang, L. Dai, F. Lu, Y. Liu, *Chem. Res. Toxicol.* **2012**, *25*, 1265 – 1270.
[28] H. Yue, W. Wei, Z. Yue, B. Wang, N. Luo, Y. Gao, D. Ma, G. Ma, Z. Su, *Biomaterials* **2012**, *33*, 4013 – 4021.
[29] Q. Mu, G. Su, L. Li, B. O. Gilbertson, L. H. Yu, Q. Zhang, Y.-P. Sun, B. Yan, *ACS Appl. Mater. Interfaces* **2012**, *4*, 2259 – 2266.
[30] Y. Li, Y. Liu, Y. Fu, T. Wei, L. Le Guyader, G. Gao, R.-S. Liu, Y.-Z. Chang, C. Chen, *Biomaterials* **2012**, *33*, 402 – 411.
[31] G.-Y. Chen, H.-J. Yang, C.-H. Lu, Y.-C. Chao, S.-M. Hwang, C.-L. Chen, K.-W. Lo, L.-Y. Sung, W.-Y. Luo, H.-Y. Tuan, Y.-C. Hu, *Biomaterials* **2012**, *33*, 6559 – 6569.
[32] A. V. Tkach, N. Yanamala, S. Stanley, M. R. Shurin, G. V. Shurin, E. R. Kisin, A. R. Murray, S. Pareso, T. Khaliullin, G. P. Kotchey, V. Castranova, S. Mathur, B. Fadeel, A. Star, V. E. Kagan, A. A. Shvedova, *Small* **2013**, DOI: 10.1002/smll.201201546.
[33] A. Sasidharan, L. S. Panchakarla, A. R. Sadanandan, A. Ashokan, P. Chandran, C. M. Girish, D. Menon, S. V. Nair, C. N. Rao, M. Koyakutty, *Small* **2012**, *8*, 1251 – 1263.
[34] K. H. Liao, Y. S. Lin, C. W. Macosko, C. L. Haynes, *ACS Appl. Mater. Interfaces* **2011**, *3*, 2607 – 2615.
[35] S. K. Singh, M. K. Singh, M. K. Nayak, S. Kumari, S. Shrivastava, J. J. A. Grácio, D. Dash, *ACS Nano* **2011**, *5*, 4987 – 4996.
[36] S. K. Singh, M. K. Singh, P. P. Kulkarni, V. K. Sonkar, J. J. Grácio, D. Dash, *ACS Nano* **2012**, *6*, 2731 – 2740.
[37] J. Yuan, H. Gao, C. B. Ching, *Toxicol. Lett.* **2011**, *207*, 213 – 221.
[38] J. Yuan, H. Gao, J. Sui, H. Duan, W. N. Chen, C. B. Ching, *Toxicol. Sci.* **2012**, *126*, 149 – 161.
[39] K. Wang, J. Ruan, H. Song, J. Zhang, Y. Wo, S. Guo, D. Cui, *Nanoscale Res. Lett.* **2011**, *6*, 1 – 8.
[40] M. Wojtoniszak, X. Chen, R. J. Kalenczuk, A. Wajda, J. Łapczuk, M. Kurzewski, M. Drozdzik, P. K. Chu, E. Borowiak-Palen, *Colloids Surf. B* **2012**, *89*, 79 – 85.
[41] W. Hu, C. Peng, W. Luo, M. Lv, X. Li, D. Li, Q. Huang, C. Fan, *ACS Nano* **2010**, *4*, 4317 – 4323.
[42] Y. Chang, S. T. Yang, J. H. Liu, E. Dong, Y. Wang, A. Cao, Y. Liu, H. Wang, *Toxicol. Lett.* **2011**, *200*, 201 – 210.
[43] H. Ali-Boucetta, D. Bitounis, R. Raveendran-Nair, A. Servant, J. Van den Bossche, K. Kostarelos, *Adv. Healthcare Mater.* **2013**, *2*, 443 – 441.
[44] X. Sun, Z. Liu, K. Welsher, J. T. Robinson, A. Goodwin, S. Zaric, H. Dai, *Nano Res.* **2008**, *1*, 203 – 212.
[45] S. Zhang, K. Yang, L. Feng, Z. Liu, *Carbon* **2011**, *49*, 4040 – 4049.
[46] X. Zhang, J. Yin, C. Peng, W. Hu, Z. Zhu, W. Li, C. Fan, Q. Huang, *Carbon* **2011**, *49*, 986 – 995.
[47] M. C. Duch, G. R. Budinger, Y. T. Liang, S. Soberanes, D. Urich, S. E. Chiarella, L. A. Campochiaro, A. Gonzalez, N. S. Chandel, M. C. Hersam, G. M. Mutlu, *Nano Lett.* **2011**, *11*, 5201 – 5207.
[48] F. A. Murphy, C. A. Poland, R. Duffin, K. T. Al-Jamal, H. Ali-Boucetta, A. Nunes, F. Byrne, A. Prina-Mello, Y. Volkov, S. Li,

S. J. Mather, A. Bianco, M. Prato, W. MacNee, K. Kostarelos, K. Donaldson, *Am. J. Pathol.* **2011**, *178*, 2587 – 2600.

[49] a) K. Kostarelos, *Nat. Biotechnol.* **2008**, *26*, 774 – 776; b) C. A. Poland, R. Duffin, I. Kinloch, A. Maynard, W. A. Wallace, A. Seaton, V. Stone, S. Brown, W. MacNee, K. Donaldson, *Nat. Nanotechnol.* **2008**, *3*, 423 – 428.

[50] K. Yang, S. Zhang, G. Zhang, X. Sun, S. T. Lee, Z. Liu, *Nano Lett.* **2010**, *10*, 3318 – 3323.

[51] A. Sahu, W. I. Choi, G. Tae, *Chem. Commun.* **2012**, *48*, 5820 – 5822.

[52] E. Zanni, G. De Bellis, M. P. Bracciale, A. Broggi, M. L. Santarelli, M. S. Sarto, C. Palleschi, D. Uccelletti, *Nano Lett.* **2012**, *12*, 2740 – 2744.

[53] W. Zhang, C. Wang, Z. Li, Z. Lu, Y. Li, J. J. Yin, Y. T. Zhou, X. Gao, Y. Fang, G. Nie, Y. Zhao, *Adv. Mater.* **2012**, *24*, 5391 – 5397.

[54] O. Akhavan, E. Ghaderi, *ACS Nano* **2010**, *4*, 5731 – 5736.

[55] a) S. Liu, T. H. Zeng, M. Hofmann, E. Burcombe, J. Wei, R. Jiang, J. Kong, Y. Chen, *ACS Nano* **2011**, *5*, 6971 – 6980; b) S. Liu, M. Hu, T. H. Zeng, R. Wu, R. Jiang, J. Wei, L. Wang, J. Kong, Y. Chen, *Langmuir* **2012**, *28*, 12364 – 12372.

[56] O. N. Ruiz, K. A. Fernando, B. Wang, N. A. Brown, P. G. Luo, N. D. McNamara, M. Vangsness, Y. P. Sun, C. E. Bunker, *ACS Nano* **2011**, *5*, 8100 – 8107.

[57] X. Cai, M. Lin, S. Tan, W. Mai, Y. Zhang, Z. Liang, Z. Lin, X. Zhang, *Carbon* **2012**, *50*, 3407 – 3415.

[58] a) I. E. M. Carpio, C. M. Santos, X. Wei, D. F. Rodrigues, *Nanoscale* **2012**, *4*, 4746 – 4756; b) C. M. Santos, J. Mangadlao, F. Ahmed, A. Leon, R. C. Advincula, D. F. Rodrigues, *Nanotechnology* **2012**, *23*, 395101.

[59] O. Akhavan, E. Ghaderi, *Carbon* **2012**, *50*, 1853 – 1860.

[60] M. Sawangphruk, P. Srimuk, P. Chiochan, T. Sangsri, P. Siwayaprahm, *Carbon* **2012**, *50*, 5156 – 5161.

[61] K. Yang, J. Wan, S. Zhang, Y. Zhang, S.-T. Lee, Z. Liu, *ACS Nano* **2011**, *5*, 516 – 522.

[62] J.-H. Liu, S.-T. Yang, H. Wang, Y. Chang, A. Cao, Y. Liu, *Nanomedicine* **2012**, *7*, 1801 – 1812.

[63] Z. M. Markovic, B. Z. Ristic, K. M. Arsikin, D. G. Klisic, L. M. Harhaji-Trajkovic, B. M. Todorovic-Markovic, D. P. Kepic, T. K. Kravic-Stevovic, S. P. Jovanovic, M. M. Milenkovic, D. D. Milivojevic, V. Z. Bumbasirevic, M. D. Dramicanin, V. S. Trajkovic, *Biomaterials* **2012**, *33*, 7084 – 7092.

[64] L. Lacerda, J. Russier, G. Pastorin, M. A. Herrero, E. Venturelli, H. Dumortier, K. T. Al-Jamal, M. Prato, K. Kostarelos, A. Bianco, *Biomaterials* **2012**, *33*, 3334 – 3343.

[65] A. V. Titov, P. Král, R. Pearson, *ACS Nano* **2010**, *4*, 229 – 334.